ADVANCES IN MATERIALS SCIENCE, Vol. 22, No. 4 (74), December 2022

sciendo

DOI: 10.2478/adms-2022-0017

Fatih Ata[1], Adnan Calık[1], Nazim Ucar[2*]

[1] *Isparta University of Applied Sciences, Faculty of Technology, Mechanical Engineering, 32260, Isparta, Türkiye*
[2] *Süleyman Demirel University, Faculty of Arts and Sciences, Department of Physics, 32260, Isparta, Türkiye*

*nazimucar@sdu.edu.tr

INVESTIGATION ON THE MICROSTRUCTURE AND MECHANICAL PROPERTIES OF ASTM A131 STEEL MANUFACTURED BY DIFFERENT WELDING METHODS

ABSTRACT

Welding is an indispensable manufacturing process in the shipbuilding industry. The fierce competition involved often necessitates a cost-effective and reliable welding method. In this study, the weldabilities, microstructures and some mechanical properties of ASTM A131 (Grade A) steel joints fabrication by submerged arc welding (SAW), metal active gas (MAG) welding and plasma arc welding (PAW) have been investigated. The microstructures of the welds were examined by optical microscopy. The mechanical properties of the joints were determined by microhardness measurements, tensile and impact tests. The results showed that tensile strength of the joints reached a tensile strength of up to 462 MPa. The locations of the fractures were always adjacent to the base metal. The Charpy impact energy of the weld metal reached a value of 72.5 J, which was 25 % higher than that of the base metal at 57.7 J. A relatively high hardness of 221 HV was obtained in the PAW method compared to 179 HV in the base metal.

Keywords: *Grade A steel; welding; tensile failure; hardness*

INTRODUCTİON

Welding is one of the most commonly used fabrication techniques in the shipbuilding industry [1-3]. Many welding methods such as electric arc welding (EAW), gas shielded arc welding (which include metal inert gas and metal active gas welding MIG/MAG, sometimes referred to as gas metal arc welding GMAW), tungsten inert gas welding (TIG, also known as gas tungsten arc welding GTAW) and submerged arc welding (SAW) are the most commonly-used joining methods for steels [4-6]. However, the characterization of the mechanical properties of the weld remains a critical concern for the safety of ship components. It has been shown that the mechanical strength of the welded joints are directly influenced by the welding process as well as process parameters which include welding current, speed, the flow rate of the shielding gas, arc voltage, etc. [7-9]. Jorge et al. [10] compared the mechanical properties of high strength steel welds obtained by shielded metal arc welding (SMAW). They showed that GMAW can be applied as an interesting alternative for the welding of high strength steels. A comprehensive study on the mechanical (tensile, impact, hardness) properties of naval grade HSLA steel joints produced by GMAW, SMAW and friction stir welding (FSW) was conducted by Nathan et al. [11]. It was concluded that FSW eliminated the problems associated with fusion welding processes and that welds produced by FSW presented superior mechanical properties compared to those produced by

GMAW and SMAW. Muthukumaran et al. [12] observed that the highest ultimate tensile strength in semi-killed steel was obtained in activated GTAW which was 2.5–5% greater than that obtained by other processes such as GMAW and GTAW, while maximum impact toughness obtained from GTAW was 50% higher than that obtained from GMAW and activated GTAW. These results were attributed to the multiple passes associated with GTAW and the formation of martensite in activated GTAW.

ASTM A131 is a low-carbon steel commonly used in shipbuilding applications [1,13,14]. Concerning the welding of these steels, Sethilkumar [15] stated that low carbon steels can be satisfactorily welded using shielded metal arc welding (SMAW). The ultimate tensile and yield strength values of the welded joints were found to increase with increasing welding current. In a related study, Boumerzoug et al. [16] reported that the microstructure of the weld metal was completely different from the heat-affected zone (HAZ) in industrial low carbon steel welded using SMAW. Maximum hardness was achieved in the HAZ due to the formation of Widmanstätten ferrite alongside large grains of ferrite and colonies of pearlite. In a study on grade A steel, Gultekin [17] observed that the weld metal and transition zone hardness of the steel welded by SAW, GMAW and electric arc welding (EAW) methods were close to each other. The hardness values in the welds were generally low due to grain coarsening caused by heat input during welding. To sum up, it can be said that the welding process can have a significant influence on the microstructure and mechanical properties of welded joints. The literature available that discusses the mechanical properties of welded ASTM A131 steel joined by different weld methods is limited. The main objective of this study is to therefore examine the weldability, mechanical properties and microstructure of ASTM A131 steel joined by three different welding methods (SAW, MAG and PAW).

MATERIALS AND METHODS

ASTM A131 steels used in this study were initially cut to dimensions of 8 mm × 150 mm × 400 mm. The chemical composition of steel was determined using optical emission spectrometer and is given in Table 1.

Table 1. *Chemical composition of Grade A steel (in wt.%)*

Material	C	Mn	P	S	Si	Cu
ASTM A131	0.16	0.55	0.012	0.012	0.18	0.02

The SAW process was performed using an ESAB LAF 1000 DC welding machine. The welding flux is selected as SA AB 1 68 AC H5 as basic character with the basicity index of 1.4 according to TS EN ISO 14174. Welding was performed using the welding wire S2 of 2.4mm in diameter according to TS EN ISO 14171-A standard (C: 0.12 / Mn: 1.0 / Si: 0.10 / Mo: 0.5/ Cu: <0.30 / copper coated). Welding parameters such as arc voltage, welding current and travel speed were selected as 30 V, 350 A and 40 cm/min, respectively. MAG/MIG welding is one of the most commonly applied welding processes in manufacturing, and in the present study, a Fronius Trans Pulse Synergic 3200 MIG welding machine was used with an Ar + 20% CO_2, 2% O_2 shielding gas. Welding parameters such as arc voltage, welding current, travel speed and shielding gas flow rate were selected as 25 V, 300 A, 30 cm/min and 12 L/min respectively. A Nermatic 450 welding machine and Argohid 5 (Ar + %5 H_2) plasma gas was used in the PAW process. The welding parameters for PAW were adjusted to 32 V, 238 A, 15 cm/min., 20 15 L/min. The welding wire SG2 of 1.2 mm in diameter according to

TS EN ISO 14171-A standard (C:0.08 / Mn:1.45 / Si:0.85) was used for MAG and PAW processes.

To measure and compare mechanical properties of welded ASTM A 131 steels, tensile, impact and Vickers microhardness tests were carried out using a 100 kN capacity servo-hydraulic MTS Landmark tester (ASTM D1822), a 300 J capacity Instron 9350 Drop Tower Charpy impact tester (ASTM E23), and a TTS Matsuzawa HWMMT-X3 microhardness tester, respectively. The Vickers microhardness measurements were made using a load of 100 g and a dwell time of 15 s (ASTM E384). Multiple indentations were made on welded surfaces to evaluate the reproducibility of the hardness data.

For microstructural characterizations, the base metal and the welded specimens were ground using different grades (400 to 1200 grit) of abrasive papers, polished with 1 μm diamond paste, and etched using a 3% Nital solution. An Olympus BX51TRF-6 optical microscope was employed to investigate microstructures of the polished and etched samples.

RESULTS AND DİSCUSSİON

The microstructure of ASTM A131 steel is presented in Figure 1a. The microstructure consists of ferrite (light matrix) and pearlite (dark phase). There is evidence of segregation, and there are inclusions present at the grain boundaries. In the literature [18], it has been reported that the microstructure of the Grade A steels used in shipbuilding are composed of ferrite and pearlite. This microstructure was also reported by Bodude and Momohjimoh [19], who stated that the structure base metal of the low carbon steel consisted of about 80–85% ferrite and 15–20% pearlite.

After welding, the weld metal region displayed significant changes compared to other zones due to recrystallization and a microstructural inhomogenity resulting from rapid cooling. Joarder et al. [20] indicated that the microstructure of the weld can vary significantly depending on the number, size and distribution of inclusions present.

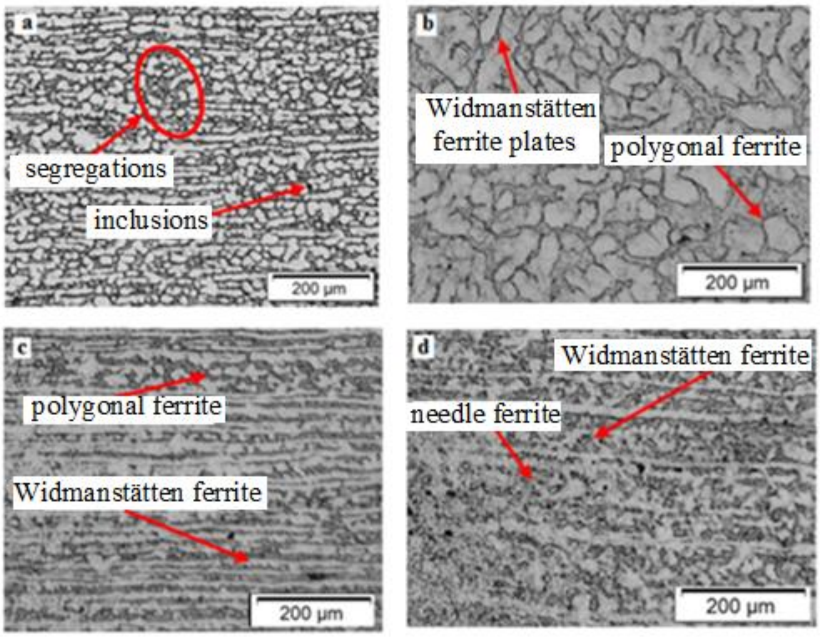

Fig. 1. Microstructure of ASTM A131 steel. Base metal (a). The weld metal region after welded with SAW (b), MAG (c), PAW (d)

Depending on energy input and cooling rates, different microstructures were formed in the welded metal zone of ASTM A 131 steel. It can be seen from Figure 1b that the microstructure in the SAW joint consisted mostly of polygonal ferrite grains and Widmanstätten ferrite plates. In the MAG weld, the microstructure also contained polygonal ferrite and Widmanstätten ferrite, but in the PAW joint the the microstructure of the weld consisted mostly of acicular ferrite with a small amount of Widmanstätten ferrite along grain boundaries (Figures 1c and d). Widmanstätten ferrite and acicular ferrite (is a needle-shaped modification of ferrite) in low carbon steel welds was also observed by Enomoto et al. [21], who noted that the lengths of the ferrite plates were controlled by carbon diffusion.

Studies on the microstructural evolution of the weld metal show that heat input and the composition of the filler metal play a very important role in the resulting microstructure of weld [11,22]. Rahul et al. [23] observed that higher heat input caused slower cooling rates leading to coarse-grained microstructures. Low heat input causes faster cooling and finer microstructures in the weld. High heat input combined with rapid cooling rates in the weld metals can lead to fine-grained polygonal ferrites at ambient temperature [24]. On the other hand, Ahangaryan et al. [25] showed that delta ferrite decreased with increasing heat input. The amount of ferrite in the samples welded using heat inputs of 0.72, 0.84 and 1.0 kJ/mm was about 13, 9 and 5%, respectively, due to relationships between heat input and cooling rate. In the present study, the heat input was calculated as 0.91, 1.33 and 3.37 kJ/mm for MAG, PAW and SAW, respectively.

In considering the microstructure of the HAZ, some grain coarsening appears to have occurred due to heat transfer in this region (Figure 2).

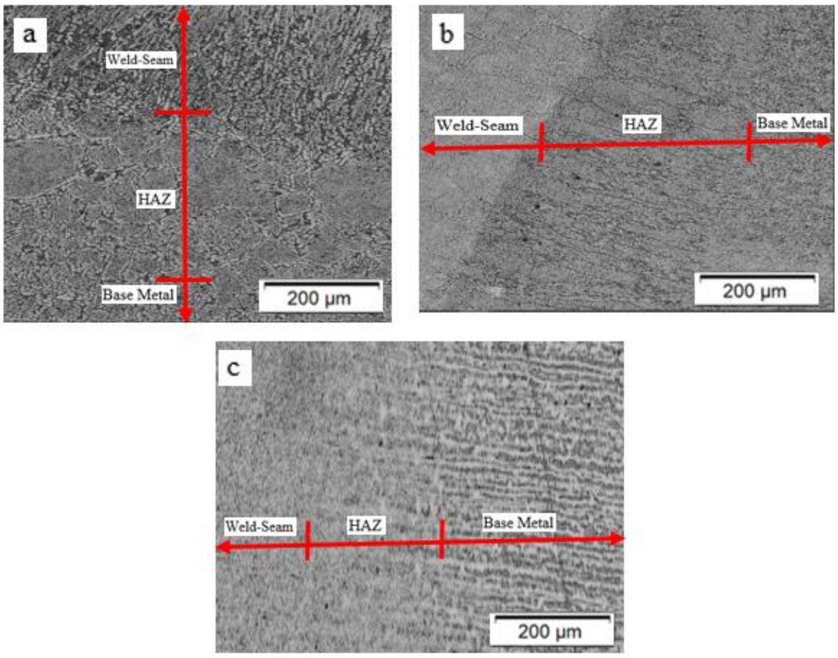

Fig. 2. Microstructures of ASTM A131 steel after welding by (a) SAW, (b) MAG, (c) PAW

Tensile tests were conducted to determine the mechanical properties of base material and welded steel. The geometry of the tensile test specimens is shown in Figure 3.

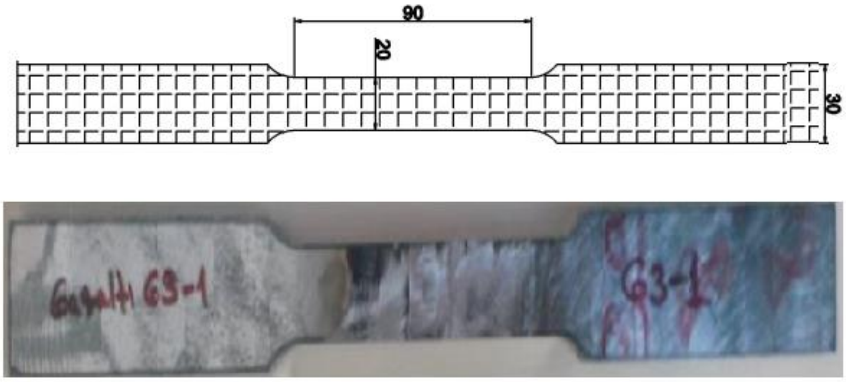

Fig. 3. Geometry and view of tensile tests specimens prepared from the welded joint. All of the dimensions provided are in mm

Images of the ASTM A131 welded joints after the tensile, bend and impact testing are shown in Figure 4 and quantitative results regarding tensile and Charpy impact tests are listed in Table 2.

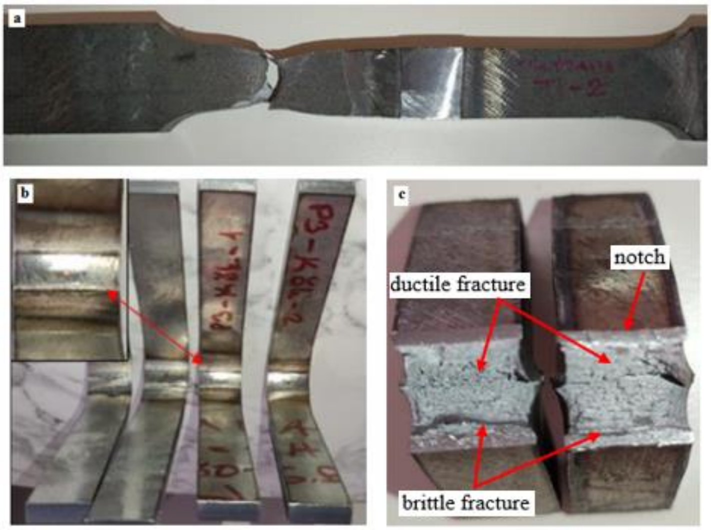

Fig. 4. Photographs of the samples after (a) tensile, (b) bend, and (c) impact testing

Table 2. *The mechanical properties of steels welded using the three different welding methods.*

Welding Method	Tensile Strength (MPa)	Yield Strength (MPa)	Elongation (%)	Impact Energy (J)
Base material	471	325	29	57.7
SAW	455	309	22	62.6
MAG	439	292	18	53.1
PAW	462	311	25	72.5

The yield, tensile strength and elongation values of the base metal were all higher compared to the welded specimens due to its uniform microstructure. Among the welded samples, the samples welded with PAW displayed the highest values of yield, tensile strength, elongation and impact energy (Table 2).

Similar results have been obtained by Bodude et al. [19] in low carbon steels welded with Oxy-Acetylene Welding (OAW) and SMAW. It was concluded in the study that as compared to SMAW, the mechanical properties of OAW was inferior due to the inherent low power density of the OAW process. In a study examining the mechanical characteristics of semi-killed steel plates using different arc welding methods, Muthukumaran et al. [12] reported that tensile failure occurred in the weld metal in the case of the GMAW/GTAW and in the base metal in the case activated GTAW due to the formation of martensite in the weld. They also noted that the joints welded using activated GTAW exhibited higher strengths compared to those welded by GMAW/GTAW.

The results of the present study show that PAW and SAW provide slightly better mechanical properties than MAG. This result can be clearly seen from Figure 5. As can be seen in the figure, tensile failure in the PAW and SAW joints occurred away from the weld, while the failure in MAG occurred close to the weld.

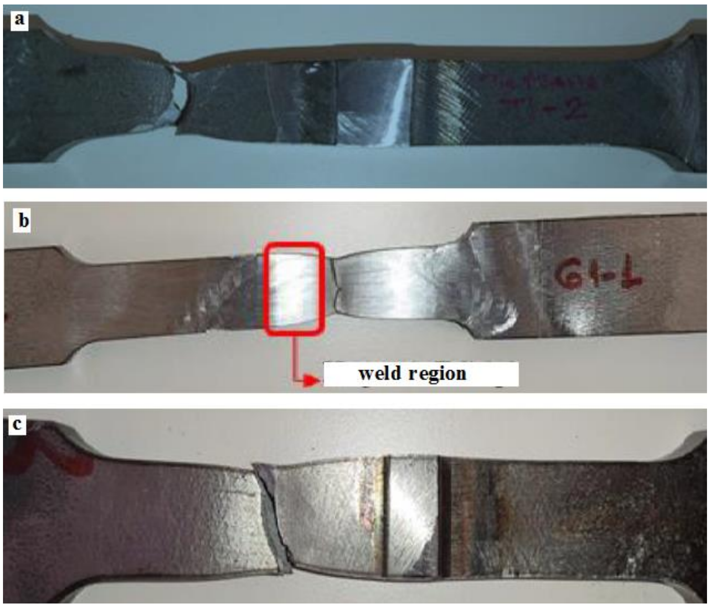

Fig. 5. Photographs showing the failure locations in the (a) SAW, (b) MAG and (c) PAW specimens

The locations of Vickers microhardness indentations made across four different regions in the cross-section of the weld are illustrated in Figure 6 and the results of the microhardness measurements are given in Table 3.

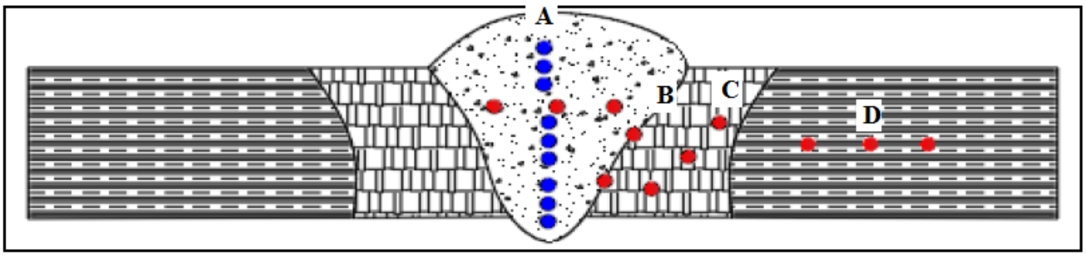

Fig. 6. Schematic illustration of the cross-section of the weld showing the four different regions on which microhardness measurements were made

Table 3. *Vickers hardness measured from different regions of cross-section of the weld as indicated in Figure 6*

Welding method	Region A	Region B	Region C	Region D
SAW	180	182	181	179
MAG	201	208	202	179
PAW	211	221	214	179

When the microhardness results were examined, it was seen that the highest hardness values were in the melting line (transition zone-region B) and the lowest values were in the base metal (Region D). This can be explained by the transfer of carbon from the base material to the weld by the influx of heat during the welding process. In addition to the carbon transfer, the sudden cooling and solidification in the region B due to the adjacent metal may have resulted in relatively high hardness values in this zone. The maximum hardness value was found to be 221 HV for PAW (Table 3). Boumerzoug et al. [16] obtained a hardness values in the range of 178–250 HV, and stated that the maximum hardness values were within the HAZ. In contrast, Gural et al. [26] found that the maximum hardness values were within of the weld metal region. In the literature [11, 20, 27-29], the variations in hardness observed in the welded parts can be attributed to several factors, mainly to residual stresses, grain size, phase composition and metallic inclusions in addition to carbon transfer during welding.

Looking at the hardness changes in the regions with welding methods, it is possible to explain the changes in terms of energy input. With increasing heat input, the likelihood of the formation of ductile phases in the regions and the hardness values decreases. As a matter of fact, the welding method with the highest energy input is SAW and the hardness value is lowest when compared to MAG and PAW. On the other hand, the highest hardness values were observed in the PAW joint. This is attributed to the formation of acicular ferrite, as observed by Kumar et al. in duplex stainless steels [30].

CONCLUSİONS

Welding of ASTM A131 steel was successfully carried out using SAW, MAG and PAW technique. The following points can be concluded from the present study:

- The base material exhibited a starting microstructure consisting of ferrite and pearlite. Significant changes in microstructure occurred as a result of heat input and cooling in the welding method.
- The heat input values were 0.91, 1.33 and 3.37 kJ/mm for MAG, PAW and SAW, respectively. The microstructure, tensile and impact properties of the welded ASTM A 131 steel were closely related to heat input associated with the welding method.
- Maximum impact energy absorption was obtained from the specimen welded with PAW while the lowest impact energy was measured in the specimen welded with MAG. The highest impact toughness, 72.5 J was partially due to high heat input during welding, which was 1.33 kJ/mm for PAW.
- Tensile failure occurred in the base metal in the case of the SAW and PAW, and occurred close to weld in the case of MAG welding. The results showed that the SAW and PAW welds were stronger compared to the MAG weld.
- The maximum hardness values were measured in the transition zone of the welded joints. The highest hardness value was found to be 221 HV using PAW welding due to the formation of acicular ferrite.

REFERENCES

1. Sirisatien T., Mahabunphachai S. and Sojiphan K, Effect of submerged arc welding process with one-side one-pass welding technique on distortion behavior of shipbuilding steel plate ASTM A131 grade A, Materials Today: Proceedings 5 (2018) 9543–9551.

2. Turan T., Kocal T. and Unlugencoglu K., Welding Technologies in Shipbuilding Industry, The Online Journal of Science and Technology 1 (2011) 1-9.
3. McPherson, N. A., Welding issues for ship structures, Journal of Marine Engineering and Technology 9 (2010) 31-41.
4. Cevik B., Analysis of Welding Groove Configurations on Strength of S275 Structural Steel Welded by FCAW, Journal of Polytechnic 21 (2018) 489-495.
5. Delzendehrooy F., Akhavan-Safar A., Barbosa A. O., Beygi R., Cardoso D., Carbas R. J. C, Marques E.A.S. and da Silva L.F.M., A comprehensive review on structural joining techniques in the marine industry, Composite Structures 289 (2022) 115490.
6. Kuril A. A., Ram G. D. J. and Bakshi S. R., Microstructure and mechanical properties of keyhole plasma arc welded dual phase steel DP600, Journal of Materials Processing Technology 270 (2019) 28–36.
7. Sarin P. and Sharma V. K., Influence of Various Process Parameters on Strength of Gas Metal Arc Welded Joints, Influence of Various Process Parameters on Strength of Gas Metal Arc Welded Joints, International Conference on Cutting Edge Technological. Challenges in Mechanical Engineering, 2017; International Advanced Research Journal in Science, Engineering and Technology 4, 3, 2017.
8. Asibeluo I. S. and Emifoniye E., Effect of Arc Welding Current on the Mechanical Properties of A36 Carbon Steel Weld Joints, International Journal of Mechanical Engineering 2 (2015) 28-37.
9. Singh G., Kumar D. and Singh A., Influence of current on microstructure and hardness of butt welding aluminium AA6082 using GTAW process, The International Journal of Mechanical Engineering Research and Technology 3 (2013) 143-146.
10. Jorge J. C. F., Monteiro J. L. D., Gomes A. J. C., Bott I. S., de Souza L. F. G., Mendes M. C. and Araújo L. S., Influence of welding procedure and PWHT on HSLA steel weld metals, Journal of Materials Research and Technology 8 (2019) 561-571.
11. Nathan S. R., Balasubramanian V., Malarvizhi S. and Rao A. G., Effect of welding processes on mechanical and microstructural characteristics of high strength low alloy naval grade steel joints, Defence Technology 11 (2015) 308-317.
12. Muthukumaran N., Kathiresan G., Shree Raam M. N., Chandru G., Dineshkumar S., Chiranjeevi K., Rajkumar S., Manikandan M. and Arulmurugan B., Comparative studies on weldability and mechanical characteristics ofsemi- killed steel using different arc welding technique, Materials Today: Proceedings 62 (2022) 5471-5476.
13. Bai Y., Chaudhari A. and Wang H., Investigation on the microstructure and machinability of ASTM A131 steel manufactured by directed energy deposition, Journal of Materials Processing Technology 276 (2020) 116410.
14. Sekban D. M., Aktaber S. M. and Purcek G., Friction Stir Welding of Low-Carbon Shipbuilding Steel Plates: Microstructure, Mechanical Properties and Corrosion Behavior, Metallurgical and Materials Transactions A 50 (2019)4127-4140.
15. Senthilkumar P., Exploration of Tensile Properties of Low Carbon Steel Welded Joint, International Journal of Scientific Research in Science, Engineering and Technology 8 (2021) 49-55.
16. Boumerzoug Z., Derfouf C. and Baudin T., Effect of Welding on Microstructure and Mechanical Properties of an Industrial Low Carbon Steel, Engineering 2 (2010) 502-506.
17. Gultekin M., 2019, Ergitmeli Kaynak Yöntemleriyle Kaynatılan Grade A Sacının İmalat Aşamasında Kaynak Bölgesinin Korozif Karakteristiği, M.Sc thesis, Gazi University.

18. Imdat K, Kaya T. and Kahraman N., An investigation on joinability of Grade A ship steel through shielded metal arc welding method in underwater and atmospheric conditions, Journal of Polytechnic 21 (2018) 543-552.
19. Bodude M. A. and Momohjimoh I., Studies on Effects of Welding Parameters on the Mechanical Properties of Welded Low-Carbon Steel, Journal of Minerals and Materials Characterization and Engineering 3 (2015) 142-153.
20. Joarder A., Saha S. C. and Ghose A. K., Study of submerged arc weld metal and heat-affected zone microstructures of a plain carbon steel, Welding Journal 70 (1991)141-146.
21. Enomoto M., K. Wu K. M., Murakami T. and Nanba S., Three dimensional observation of ferrite plain low carbon steel weld, ISIJ International 45 (2005)756-762.
22. DuPont J. N., Microstructural evolution and high temperature failure of ferritic to austenitic dissimilar welds, International Materials Reviews 57 (2012) 3-28.
23. Kumar R. I., Arya H. K. and Saxena, R., Experimental Determination of Cooling Rate and its Effect on Microhardness in Submerged Arc Welding of Mild Steel Plate (Grade c-25 as per IS 1570), Journal of Material Sciences and Engineering 3 (2014) 1-4.
24. Gharibshahiyan E., Raouf A. H., Parvin N. and Rahimian M., The effect of microstructure on hardness and toughness of low carbon welded steel using inert gas welding, Materials and Design 32 (2011) 2042-2048.
25. Ahangaryan M., Jafarzadegan M. and Taghiabadi R., Heat Input Effect on Microstructure and Mechanical Properties in Shielded Metal Arc Welding of Dissimilar AISI 316L/St-37 Steel, International Journal of ISSI 17 (2020) 1-10.
26. Gural A., Bostan B. and Ozdemir A. T., Heat Treatment in Two Phase Region and its Effect on Welding of a Low Carbon Steel, Materials and Design 28 (2007) 897-903.
27. Sun Y. L., Hamelin C. J., Vasileiou A. N., Xiong Q., Flint T. F., Obasi G., Francis J. A and Smith M. C., Effects of dilution on the hardness and residual stresses in multipass steel weldments, International Journal of Pressure Vessels and Piping 187 (2020) 104154.
28. Sawanishi C., Matsuda H., Tagawa T., Ikeda R and Tsutsumi S., Influence of shape of weld toe and hardness of weld metal on fatigue properties in GMA welded fillet lap joint of UHSS sheet, Welding International 34 (2020) 375-387.
29. Nitsche A., Solidification phenomena in creep resistant 9Cr weld metals and their implications on mechanical properties, Welding in the World 64 (2020) 633–645.
30. Kumar T. V., Karthick K., Dhanushkaran K and Jagadeesh D., Optimising the parameters and increasing the hardness of duplex stainless steel by annealing process in valve manufacturing industries, IOP Conference Series: Materials Science Engineering 954 (2020) 012005.